Molecular Therapy
Nucleic Acids
Original Article

circNrxn2 Promoted WAT Browning via Sponging miR-103 to Relieve Its Inhibition of FGF10 in HFD Mice

Tiantian Zhang,[1] Zhenzhen Zhang,[1] Tianyu Xia,[1] Chenlong Liu,[1] and Chao Sun[1]

[1]College of Animal Science and Technology, Northwest A&F University, Yangling, Shaanxi 712100, China

The accumulation of excess white adipose tissue (WAT) has harmful consequences on metabolic health. WAT browning confers beneficial effects on adiposity, insulin resistance, and hyperlipidemia. In this study, it was found out that circNrxn2 sponged miR-103 and enhanced FGF10 levels in HFD mice WAT. We discovered that circNrxn2 promoted WAT browning and mitochondria functions. Furthermore, circNrxn2 also increased M2 macrophage polarization in HFD mouse adipose tissue, and the PPARγ signaling pathway participated in these biological processes. Moreover, eliminating adipose tissue macrophages (ATMs) by clodronate-crippled circNrxn2 promoted WAT browning, and the simulation co-culture of macrophages and adipocytes results suggested that circNrxn2 promoted WAT browning through increasing M2 macrophage polarization. Our finding revealed that circNrxn2 acted as an endogenous miR-103 sponge, blocked miR-103 effects, and relieved its inhibition of FGF10 expression to promote WAT browning through increasing M2 macrophage polarization. This study provides a good therapeutic strategy for treating obesity and improving obesity-related metabolic disorders.

INTRODUCTION

Due to the improvement of living and the change of lifestyles, the number of people with obesity in China has seen explosive growth in recent years. The accumulation of excess white adipose tissue (WAT) is the main reason of obesity. Brown adipose tissue (BAT), which is different from WAT, can burn fat and promote energy metabolism, thus providing new methods for the prevention of obesity and associated metabolic diseases.[1] WAT from certain depots, in response to appropriate stimuli, can undergo a process known as browning that takes on characteristics of BAT—notably, the induction of uncoupling protein 1 (UCP1) expression and the presence of multilocular lipid droplets and multiple mitochondria.[2]

Except for adipocytes, adipose tissue also contains abundant adipose tissue macrophages (ATMs).[3] There are two phenotypes of ATMs. In obesity, a large number of pro-inflammatory M1 macrophages recruited in adipose tissue release amounts of inflammation factors and lead to chronic inflammation and metabolic disorders.[4] There exists a dynamic conversion in the proportion of M1 and M2 macrophages, which is closely related to adipose metabolism and energy expenditure.[5,6] It has been reported that the transformation of M1 to M2 macrophages promoted the activation of BAT and the browning of WAT.[7,8] Because PPARγ plays a key role in M2 polarization and in the browning of white adipocytes, and in macrophage polarization in association with its browning capacity, we hypothesize that circNrxn2-miR-103-FGF10 could also affect WAT browning by affecting macrophage polarization.

Circular RNAs (circRNAs) are a group of non-coding RNAs (ncRNAs) characterized by the presence of a covalent bond linking 3′ and 5′ ends produced by backsplicing.[9,10] circRNAs are widely spread with stable structures, conserved sequences, and cell- or tissue-specific expression.[11] Studies have shown that circRNAs can function in multiple ways. They can act as a natural microRNA (miRNA) sponge to regulate miRNA expressions or regulate gene transcription, cell cycle, and other physiological processes through interaction with proteins. ciRS-7/CDR1as has been identified as a miR-7 sponge to inhibit miR-7 activity.[12] Wang and colleagues[13] found that a heart-related circRNA (HRCR), which acted as a miR-223 sponge, was correlated with pathological hypertrophy and heart failure. These studies are strongly supported by the idea that circRNAs can be used as a biomarker for disease diagnosis. However, their functions are still largely unidentified and have broad research prospects, and whether there exist circRNAs acting as a miR-103 sponge has not been studied.

miRNAs are a class of small (18–25 nt) single-stranded ncRNAs that function as endogenous regulators by targeting mRNAs.[14] miRNA dysfunction is related to a variety of human diseases, such as obesity and metabolic disorders, suggesting that miRNAs play vital roles in obesity.[15,16] Aberrant expressions of miRNAs, including miR-221, miR-519d, miR-141, and miR-520e, are associated with human obesity and related metabolic syndrome.[17–19] Among them, miR-103 belongs to a highly conserved family of miRNA and is abundant in adipose tissue.[20,21] Dozens of miR-103 target genes, such as Dicer,

Received 22 February 2019; accepted 22 June 2019;
https://doi.org/10.1016/j.omtn.2019.06.019.

Correspondence: Chao Sun, College of Animal Science and Technology, Northwest A&F University, Yangling, Shaanxi 712100, China.
E-mail: sunchao2775@163.com

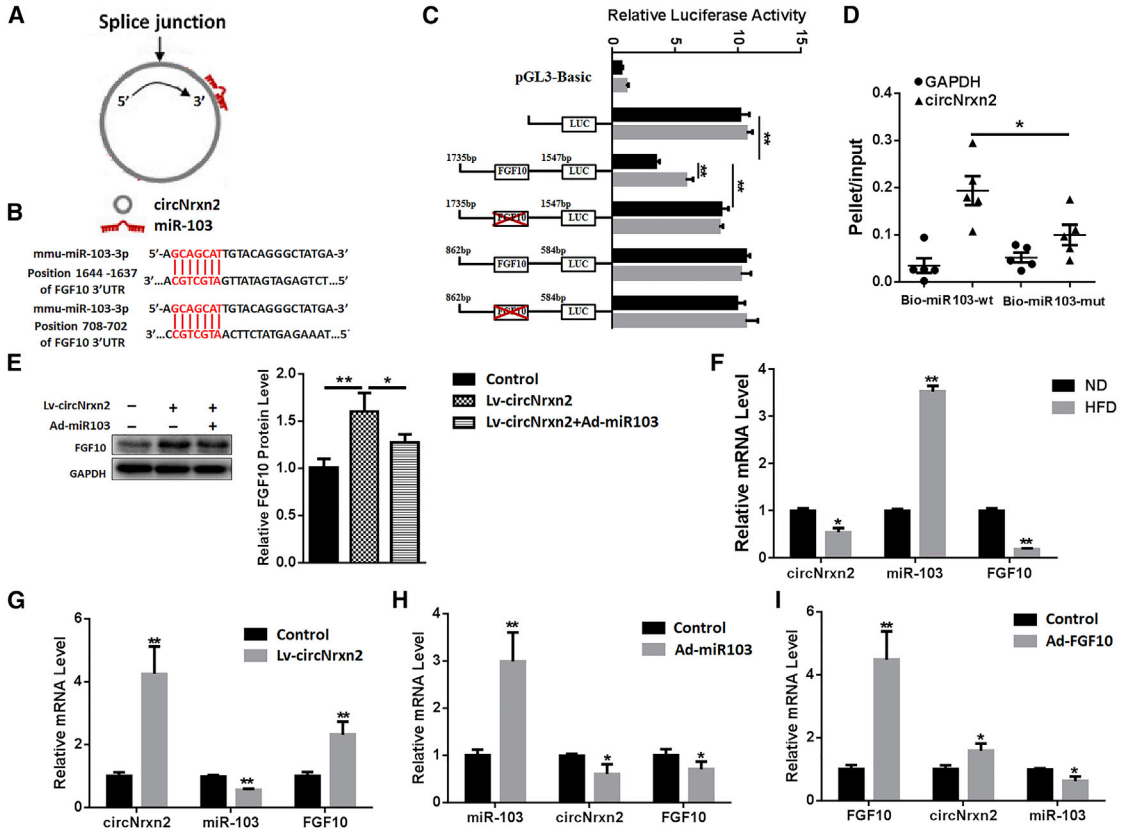

Figure 1. circNrxn2 Acted an Endogenous miR-103 Sponge and Increased FGF10 Expression in Mice Adipose Tissue

(A) Scheme of the interaction of circNrxn2 and miR-103. (B) Scheme of the interaction of miR-103 and FGF10. (C) Double luciferase assay was performed. (D) qRT-PCR was used to detected circNrxn2 and GAPDH levels after streptavidin capture. (E) The expression of FGF10 in WAT of HFD mice (8-week-old C57BL/6J mice fed with an HFD for 10 weeks; inguinal WAT (iWAT) was acquired for these experiments). (F) The expression of circNrxn2, miR-103, and FGF10 in iWAT of HFD mice. (G–I) The expressions of circNrxn2 (G), miR-103 (H), and FGF10 (I) in iWAT of HFD mice after circNrxn2, miR-103, or FGF10 treatment. Data represent the mean ± SEM. *$p < 0.05$; **$p < 0.01$. $n \geq 3$.

Cav1, DAPK, KLF4, Fadd, Mef2d, and Wnt3a, have been demonstrated to regulate adipogenesis, insulin sensitivity, cell migration, metastasis, and apoptosis.[21–27] However, the regulation of miR-103 in ATMs and WAT browning has not been studied.

In this study, we present that circNrxn2, miR-103, and FGF10 formed a regulatory circuit in adipose tissue and that they regulated WAT browning by ATM polarization. This study provides a molecular basis for preventing obesity and obesity-associated metabolic disorders.

RESULTS

circNrxn2 Acted as an Endogenous miR-103 Sponge and Increased FGF10 Expression in HFD Mice Adipose Tissue

To search for circRNAs and mRNAs that bind to miR-103, bioinformatics were carried out for predictive analysis. Among the numerous molecules, there is a potential binding site for miR-103 in the circ005661 sequence, which we called circNrxn2, as it was transcribed from the Nrxn2 gene (Figure 1A), and there are two binding sites for miR-103 in the 3′ UTR of FGF10 mRNA (Figure 1B). Therefore, circNrxn2 and FGF10 were selected as candidate molecules that interacted with miR-103. A dual luciferase reporter assay was conducted, and we found that overexpressing miR-103 caused a significant decrease in the luciferase activity of the 3′ UTR FGF10 (1,637–1,644), whereas there was no difference between the 3′ UTR FGF10 (702–708) and the control group (Figure 1C). Moreover, the mutation of 3′ UTR FGF10 (1,637–1,644) displayed no difference from the control group (Figure 1C). The data suggested that FGF10 (1,637–1,644) may be the potential binding site for miR-103.

In addition, circNrxn2 was added to the luciferase activity assay system. It was found that circNrxn2 addition increased the luciferase activity compared to the relative control group (Figure 1C), meaning that circNrxn2 relieved the inhibitory effect of miR-103 on FGF10. Besides, circNrxn2 was much more enriched in the miR-103-captured fraction compared with the corresponding mutant group (Figure 1D). Western blot analysis also indicated that circNrxn2 treatment upregulated the FGF10 protein level and that the addition of miR-103 reversed it (Figure 1E). A high-fat diet (HFD) upregulated the miR-103 level, while circNrxn2 and

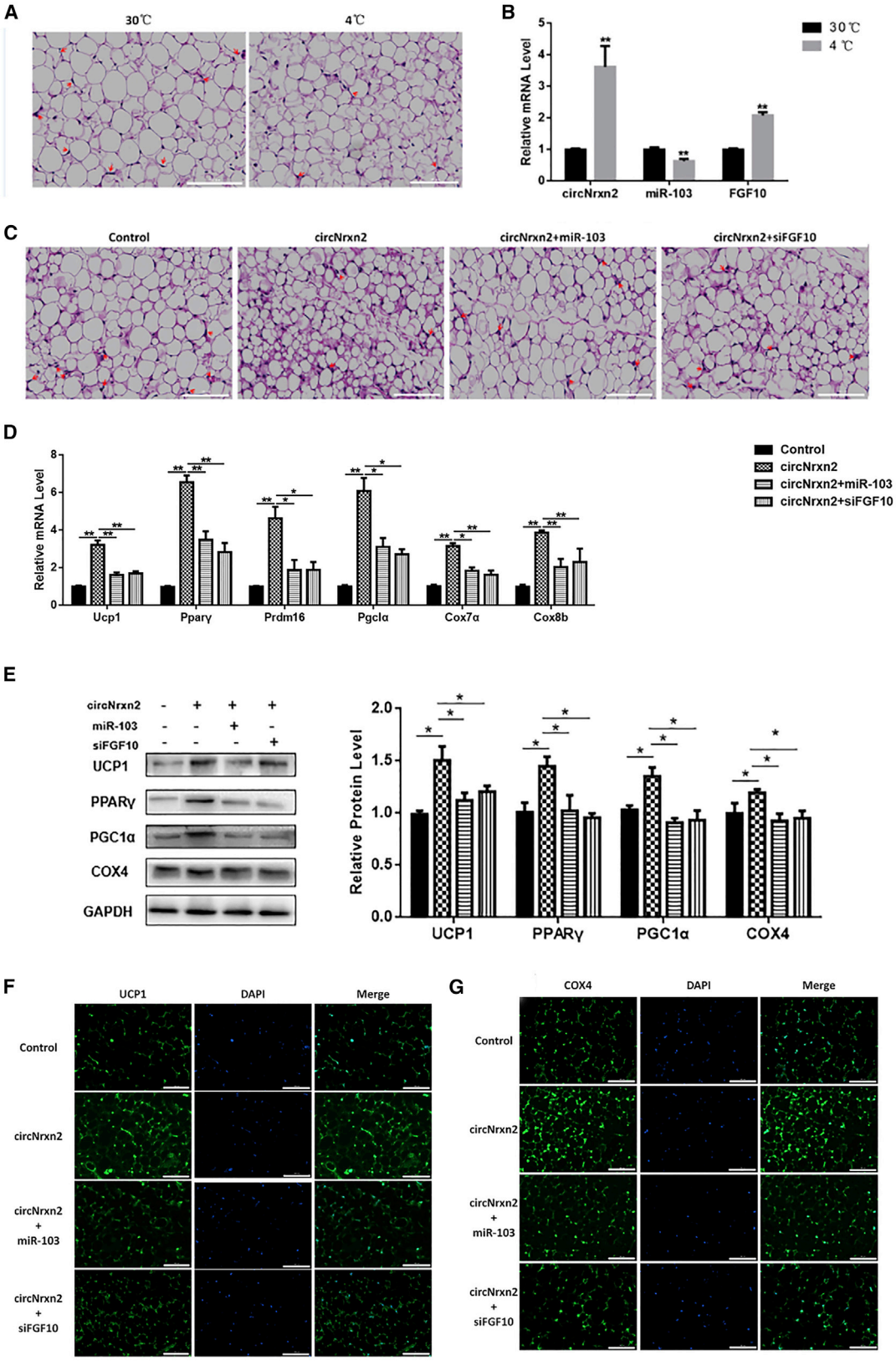

(legend on next page)

FGF10 levels were lower in the adipose tissue of HFD mice than that in normal diet (ND) mice (Figure 1F). These results confirmed that circNrxn2 could sponge miR-103, thus crippling the effect of miR-103 on FGF10.

To avoid the effects of expression vectors on other tissues, we used adipose-tissue-specific expression vectors and evaluated their expression in liver, muscle, perirenal fat, WAT, and BAT (Figures S1A–S1C). HFD mice were injected intraperitoneally (i.p.) with the circNrxn2 miR-103 and FGF10 viruses, respectively. It was found that circNrxn2 significantly decreased the miR-103 level and increased the FGF10 mRNA level (Figure 1G). miR-103 overexpression inhibited circNrxn2 and FGF10 mRNA levels (Figure 1H). FGF10 treatment enhanced circNrxn2 and inhibited miR-103 levels (Figure 1I). These results indicated that circNrxn2 acted as an endogenous miR-103 sponge and increased FGF10 expression in mouse adipose tissue.

circNrxn2 Promoted WAT Browning in HFD Mice

To investigate the roles of circNrxn2-miR103-FGF10 in WAT browning, HFD mice were housed at 4°C for 12 h. Cold stimulation led to smaller adipocytes and less crown structure as reported previously (Figure 2A).[28] Cold stimulation upregulated circNrxn2 and FGF10 levels and downregulated the miR-103 level significantly (Figure 2B), indicating that circNrxn2-miR-103-FGF10 had a potential role in WAT browning. HFD mice were injected i.p. with circNrxn2 lentivirus, circNrxn2 lentiviruses + miR-103 adenoviruses, circNrxn2 lentiviruses + short interfering (si)FGF10 lentiviruses, or control empty viruses. We found that the size of adipocytes was decreased after circNrxn2 treatment and that the addition of miR-103 or siFGF10 abolished the effect of circNrxn2 (Figure 2C). Also, the temperature of mice treated with circNrxn2 was significantly increased (Figure S1D). qRT-PCR was used to detect the effect of circNrxn2-miR-103-FGF10 on WAT browning. We found that circNrxn2 facilitated the mRNA levels of UCP1, PPARγ, PRDM16, PGC1α, COX7α, and COX8b (Figure 2D; Figures S1E, S1F, and S2) and the protein levels of UCP1, PPARγ, PGC1α, and COX4 (Figure 2E), indicating that circNrxn2 promoted WAT browning, mitochondrial synthesis, and oxidation. In addition, miR-103 or siFGF10 addition reversed the effect of circNrxn2 (Figures 2D and 2E). Immunofluorescent staining also showed that circNrxn2 increased the expressions of UCP1 and COX4 (Figures 2F and 2G), and the addition of miR-103 or siFGF10 reversed it. These data suggested that FGF10 promoted WAT browning, mitochondrial synthesis, and oxidation, while miR-103 and siFGF10 inhibited it. circNrxn2-miR-103-FGF10 had a vital role in WAT browning.

To further explore the roles of circNrxn2-miR-103-FGF10 in regulating white adipocytes browning, adipocytes were treated with circNrxn2, circNrxn2 + miR-103, circNrxn2 + siFGF10, or control empty viruses, respectively, and then incubated with CL316, 243 to induce white adipocytes browning. Consistent with the results *in vivo*, circNrxn2 treatment increased the transcriptional and post-transcriptional levels of PRDM16, PPARγ, and PGC1α (Figure 3A). Besides, circNrxn2 promoted the mRNA levels of Cox7α and Cox8b (Figure 3A) and the protein levels of Cox4, PPARγ and PGC1α (Figure 3B), and these effects were reversed after the addition of miR-103 or siFGF10 (Figures 3A and 3B). Moreover, we found that circNrxn2 increased the mitochondrial number and that the addition of miR-103 or siFGF10 decreased it (Figures 3C and 3D). Immunofluorescent staining also showed that circNrxn2 promoted UCP1 expression and that miR-103 or siFGF10 addition decreased it (Figure 3E). These results indicated that FGF10 could promote WAT browning and mitochondrial function, whereas miR-103 and siFGF10 have opposite effects.

circNrxn2 Increased M2 Macrophage Polarization in Mice

We had found that circNrxn2 decreased crown structure in adipose tissue (Figure 2C). ATM phenotypic conversion could regulate energy metabolism and BAT activation, so we detected the influence of circNrxn2 on ATM polarization. We found that circNrxn2 treatment promoted the expression of CD206, an M2 macrophage marker, and it was reversed after the addition of miR-103 adenoviruses or siFGF10 (Figure 4A). In addition, circNrxn2 upregulated the mRNA levels of interleukin (IL)-4 and CD206 and decreased IL-6 and tumor necrosis factor α (TNF-α) mRNA levels (Figure 4B), which were abolished after the addition of miR-103 or siFGF10 (Figure 4B). These results suggested that circNrxn2 and FGF10 promoted M2 macrophage polarization and that miR-103 inhibited M2 macrophage polarization *in vivo*.

In order to examine the effects of circNrxn2-miR-103-FGF10 on macrophage polarization, we isolated and cultivated macrophages *in vitro* and then treated them with circNrxn2, circNrxn2 + miR-103, circNrxn2 + siFGF10, or control empty viruses. It was found that circNrxn2 promoted the mRNA levels of IL-4 and CD206 (Figure 4C) and the protein levels of IL-10 and CD206 (Figure 4D). In addition, the mRNA and protein levels for M1 macrophage markers IL-6 and TNF-α were decreased after circNrxn2 treatment (Figures 4C and 4D) and were reversed after the addition of miR-103 and siFGF10 (Figures 4C and 4D). Immunofluorescent staining results also showed that circNrxn2 increased CD206 expression and that the addition of miR-103 or siFGF10 decreased it (Figure 4E). Besides, the macrophages were mostly circular after circNrxn2 treatment and

Figure 2. circNrxn2 Promoted WAT Browning in HFD Mice

HFD mice were 8-week-old C57BL/6J mice fed with an HFD for 10 weeks. They were injected i.p. with circNrxn2 lentivirus, circNrxn2 lentiviruses + miR-103 adenoviruses, circNrxn2 lentiviruses + siFGF10 lentiviruses, or control empty viruses. (A) H&E staining of adipose tissue section. (B) The changes of circNrxn2, miR-103, and FGF10 after cold stimulation. (C) H&E staining of adipose tissue section after circNrxn2, circNrxn2+miR-103, circNrxn2+siFGF10, or control treatment. (D) The relative mRNA levels of UCP1, PPARγ, PRDM16, PGC1α, COX7α, and COX8b of iWAT after circNrxn2, circNrxn2+miR-103, or circNrxn2+siFGF10 treatment in HFD mice. (E) Western blot analysis of protein levels of UCP1, PPARγ, PGC1α, and COX4 in WAT. (F and G) Immunofluorescent staining of (F) UCP1 and (G) Cox4 in adipocytes under circNrxn2, circNrxn2+miR-103, or circNrxn2+siFGF10 treatment. Data represent the mean ± SEM. Scale bars, 100 μm. *$p < 0.05$; **$p < 0.01$. $n \geq 3$.

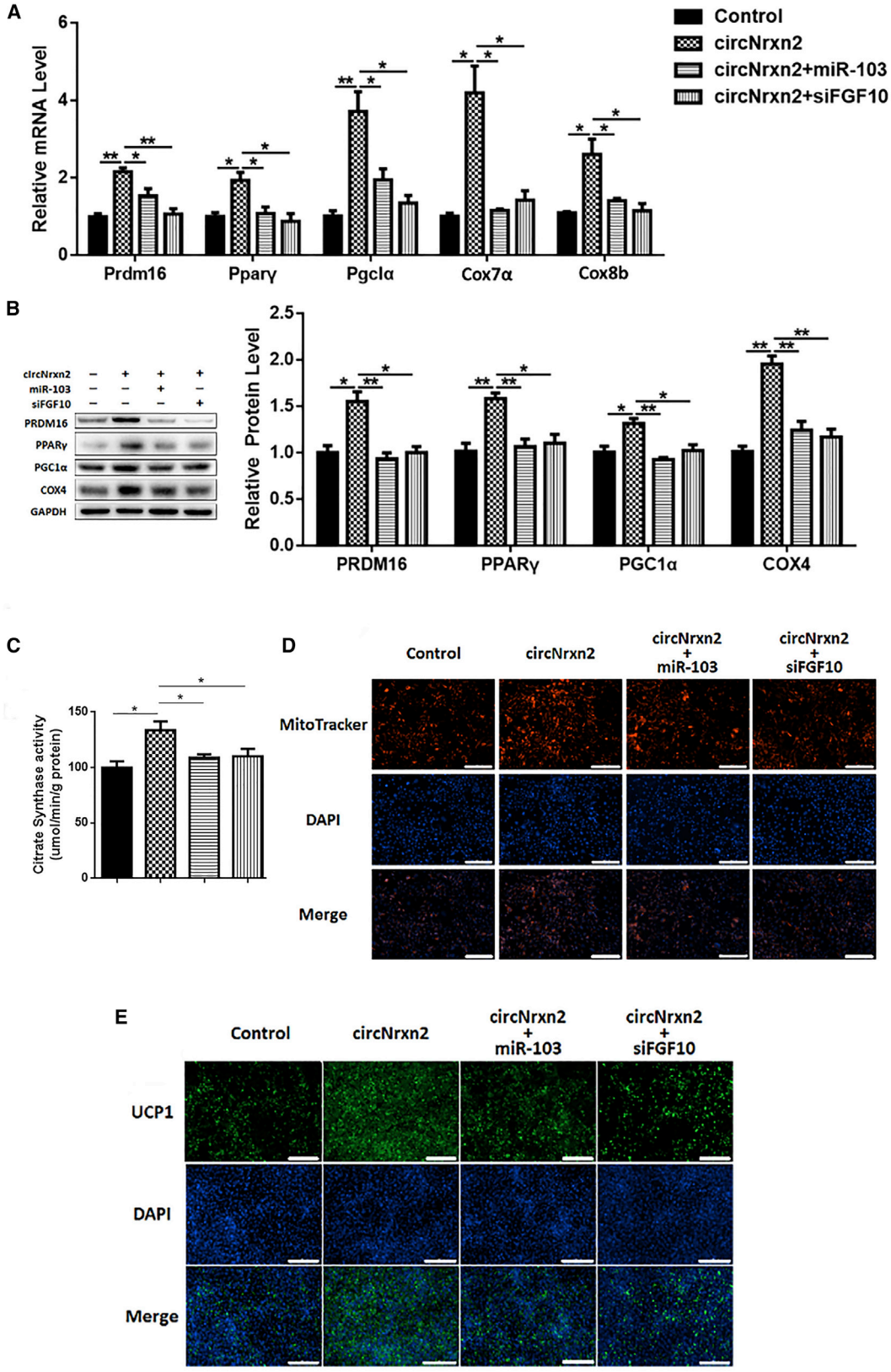

(legend on next page)

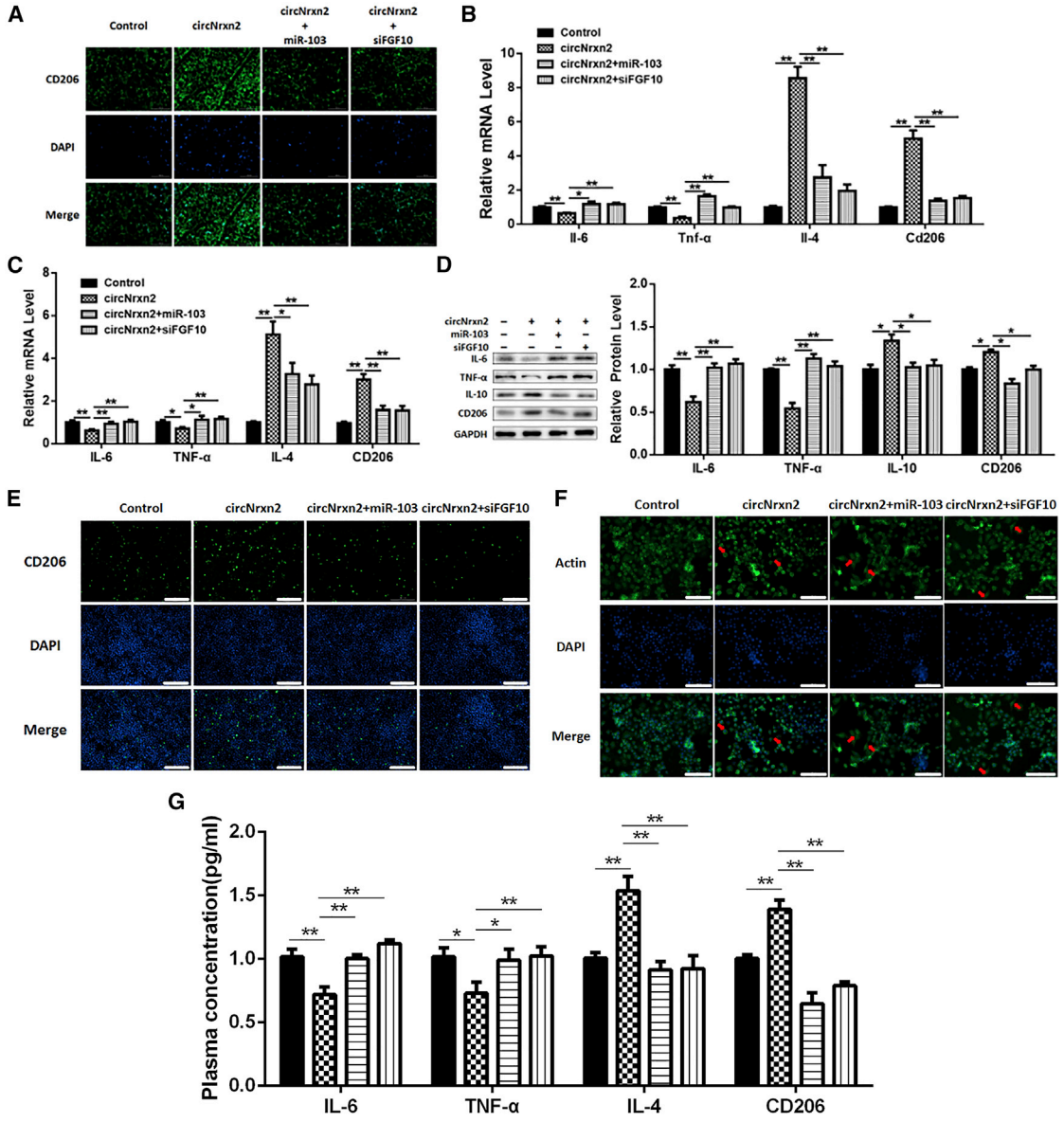

Figure 4. circNrxn2 Increased M2 Macrophage Polarization in HFD Mice

(A) CD206 immunofluorescent staining of HFD mice adipose tissue section. (B) The mRNA levels of IL-6, TNF-α, IL-4, and CD206 in adipose tissue. (C) The mRNA levels of IL-6, TNF-α, IL-4, and CD206 in macrophages. (D) The protein levels of IL-6, TNF-α, IL-10, and CD206 in macrophages. (E) Immunofluorescent staining of CD206. (F) The morphologic observation of macrophages. (G) The mRNA levels of IL-6, TNF-α, IL-4, and CD206 in plasma were detected to evaluate the systemic effects of circNrxn2, miR-103, and FGF10. Data represented the mean ± SEM. Scale bars, 200 μm. *$p < 0.05$; **$p < 0.01$. $n \geq 3$.

exhibited spindle type after adding miR-103 or siFGF10 (Figure 4F). To evaluate the systemic effects of circNrxn2, miR-103, and FGF10, the expression of IL-6, TNF-α, IL-4, and CD206 in plasma of mice was measured (Figure 4G). These results all indicated that circNrxn2 treatment induced M2 macrophage polarization, which was blocked after the addition of miR-103 or siFGF10.

Figure 3. circNrxn2 Promoted White Adipocytes Browning *In Vitro*

3T3-L1 adipocytes were treated with circNrxn2, circNrxn2 + miR-103, circNrxn2 + siFGF10, or control empty viruses. (A) The relative mRNA levels of PRDM16, PPARγ, PGC1α, COX7α, and COX8b. (B) The protein levels of PRDM16, PPARγ, PGC1α, and COX4. (C) The mitochondria staining with mitochondrial tracker. (D) The citrate synthase activity was detected in adipocytes under treatment of circNrxn2, circNrxn2 + miR-103, and circNrxn2 + siFGF10. (E) Immunofluorescent staining of UCP1 in adipocytes. Data represent the mean ± SEM. Scale bars, 200 μm. *$p < 0.05$; **$p < 0.01$. $n \geq 3$.

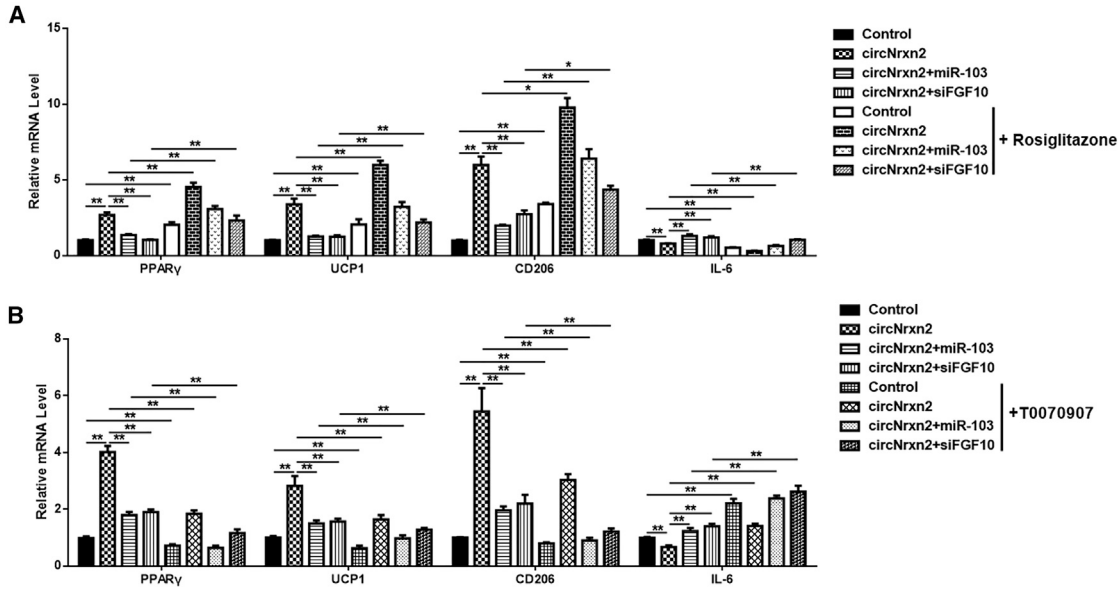

Figure 5. circNrxn2 Promoted WAT Browning and Increased M2 Macrophage Polarization by Activating the PPARγ Signaling Pathway

(A and B) PPARγ agonist (A) and antagonist (B) were injected in HFD mice adipose tissue combined with circNrxn2, miR-103, and FGF10 after circNrxn2, miR-103, or FGF10 treatment. The mRNA levels of PPARγ, UCP1, CD206, and IL-6 were detected. Data represented the mean ± SEM. *p < 0.05; **p < 0.01. n ≥ 3.

circNrxn2 Promoted WAT Browning and Increased the M2 Macrophage Polarization by Activating PPARγ Signaling Pathway

It has been reported that PPARγ signaling is essential in regulating WAT browning and ATM polarization.[29,30] We found that circNrxn2 activated PPARγ expression in mouse adipose tissue, so we tried to explore whether the PPARγ signaling pathway participated in circNrxn2 regulation of WAT browning and ATM polarization. PPARγ agonist and antagonist were used to treat mouse adipose tissue. The results showed that Rosiglitazone, a PPARγ agonist, enhanced circNrxn2-induced PPARγ, UCP1, and CD206 and blocked circNrxn2-inhibited IL-6 (Figure 5A). Besides, miR-103 and siFGF10 addition suppressed the effects of circNrxn2, and Rosiglitazone treatment also enhanced these effects (Figure 5A). Furthermore, T0070907, a PPARγ antagonist, was used to verify our results. We found that T0070907 restrained circNrxn2-induced PPARγ, UCP1, and CD206 and increased circNrxn2-inhibited IL-6 (Figure 5B). T0070907 treatment also enhanced the effects of the addition of miR-103 and siFGF10 (Figure 5B). These results suggested that circNrxn2 promoted WAT browning and increased M2 ATM polarization by activating the PPARγ signaling pathway.

circNrxn2 Promoted WAT Browning by Increasing M2 Macrophage Polarization in HFD Mice

To further explore the relationship between circNrxn2-miR-103-FGF10-regulated ATM polarization and WAT browning, clodronate was used to eliminate macrophages. As a result, it was found out that clodronate treatment efficiently decreased F4/80 expression in WAT of HFD mice (Figure 6A). Although circNrxn2 promoted the mRNA levels of UCP1, DIO2, PPARγ, COX7α, COX8b, and PGC1α, the addition of miR-103 or siFGF10 caused the downregulation of these factors (Figures 6B and 6C), and clodronate treatment decreased the degree of WAT browning regulated by circNrxn2-miR-103-FGF10 (Figures 6B and 6C). Similar results were found in western blot analysis, which also showed that circNrxn2 induced less upregulation of PRDM16, UCP1, PPARγ and COX4 and that the addition of miR-103 or siFGF10 also reduced gene expression after clodronate treatment (Figure 6D). These results indicated that the circNrxn2-miR-103-FGF10-regulated WAT browning was partially achieved by ATM polarization.

Furthermore, macrophages were treated with circNrxn2, circNrxn2 + miR-103, circNrxn2 + siFGF10, or control empty viruses, and then the supernatants were collected and added to culture adipocytes. The results showed that circNrxn2 treatment resulted in an increase in the mRNA levels of PRDM16, UCP1, PPARγ, PGC1α, COX7α and COX8b, while the addition of miR-103 or siFGF10 inhibited the expression of these genes (Figure 7A). Western blot also showed that circNrxn2 treatment increased the protein levels of PRDM16, UCP1, PPARγ, PGC1α and COX4, and that miR-103 or siFGF10 addition reversed the effects (Figure 7B), which was consistent with UCP1 immunofluorescence results (Figures 7C). These data indicated that circNrxn2-miR-103-FGF10 promoted WAT browning by increasing M2 macrophage polarization.

DISCUSSION

The location of the different types of adipose tissue varies. BAT is mainly distributed in subscapular and interscapular tissue and around the kidneys, and beige adipose tissue and WAT mainly exist in subcutaneous and internal organs of mice.[31] Under appropriate

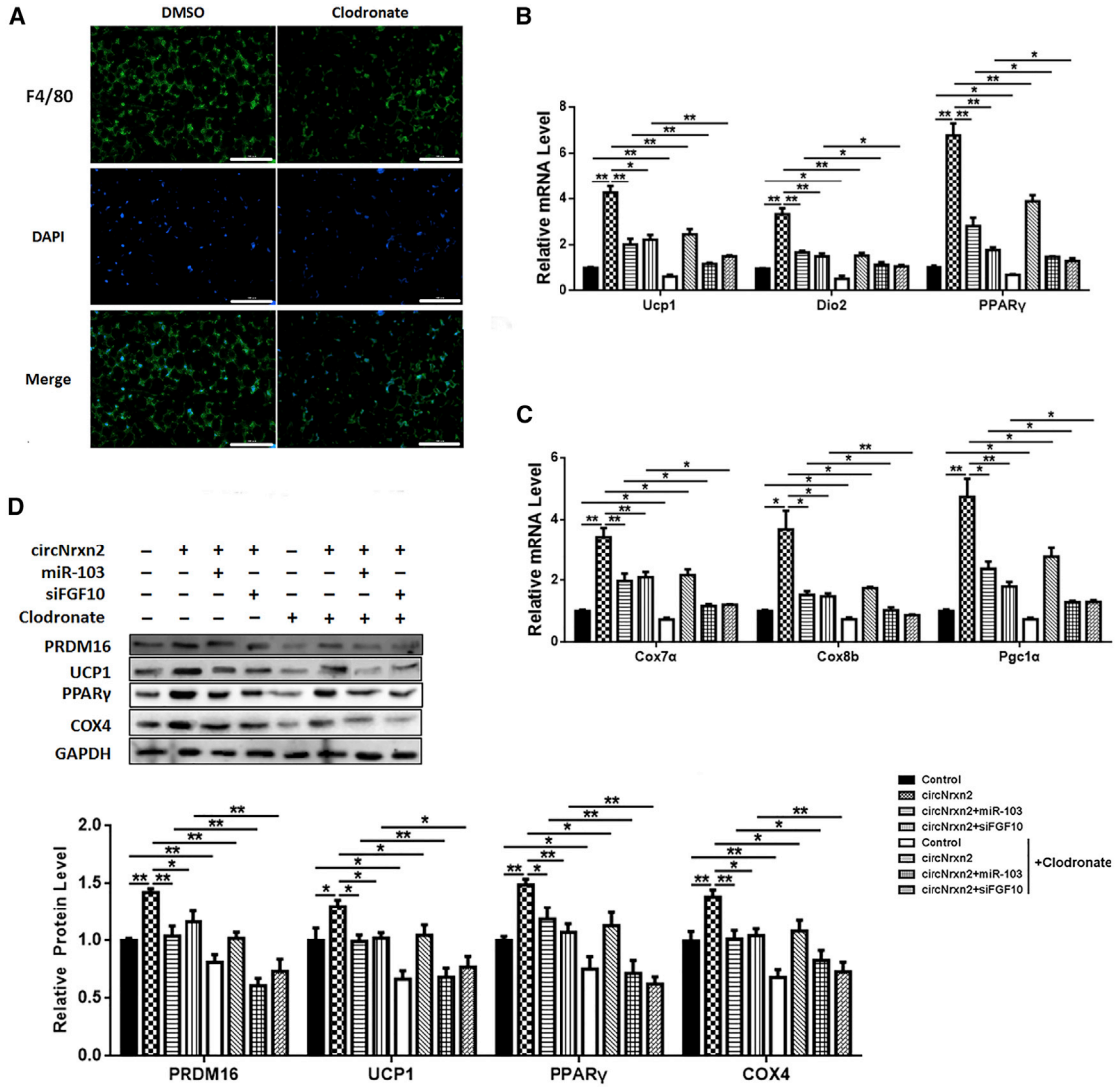

Figure 6. circNrxn2 Promoted WAT Browning by Increasing M2 Macrophage Polarization in HFD Mice

HFD mice were treated with clodronate to eliminate macrophages. (A) Immunofluorescent staining of F4/80 in HFD mouse adipose tissue after clodronate treatment. (B and C) The mRNA levels of (B) UCP1, DIO2, and PPARγ and of (C) PGC1α, COX7α, and COX8b. (D) The protein levels of PRDM16, PPARγ, and COX4. Data represent the mean ± SEM. Scale bars, 200 μm. *$p < 0.05$; **$p < 0.01$. $n \geq 3$.

stimulations, such as cold exposure, β-3 adrenergic receptor agonists, and thiazolidinediones, white adipocytes can be transformed into thermogenic adipocytes with higher UCP1 expression like BAT. This process is called browning.[32] Many studies have found that a variety of stimuli and factors, such as miRNA, macrophages, and certain drugs, can regulate WAT browning, which is more likely to occur in the inguinal WAT (iWAT).[33–35] Besides, PPARγ is widely studied as a classical factor regulating browning. In this paper, the work we did is also on these bases.

circRNAs serve as endogenous miRNA sponges to influence the expression of downstream miRNA target genes. For example, ciRS-7/CDR1as binds miR-7 to sequester away miR-7, resulting in high-level expression of target genes.[12,36] miR-103 has been confirmed to play a critical role in lipid metabolism; it was proved that miR-103 can promote 3T3-L1 cell differentiation and regulate insulin sensitivity.[21,25] Furthermore, genome-wide approaches also identified that miR-103 could bind with PPARγ.[37] Consistent with these findings, our research displays that circNrxn2 acts as a miR-103 sponge to enhance the FGF10 level, thus promoting WAT browning.

Different miRNA types and their effects have also been studied in WAT browning and adipose tissue regulation. Various kinds of miRNAs have been shown to regulate subcutaneous WAT browning and BAT activation in cold exposure. A previous study has shown that miR-32 inhibition reduces FGF21 expression to decrease

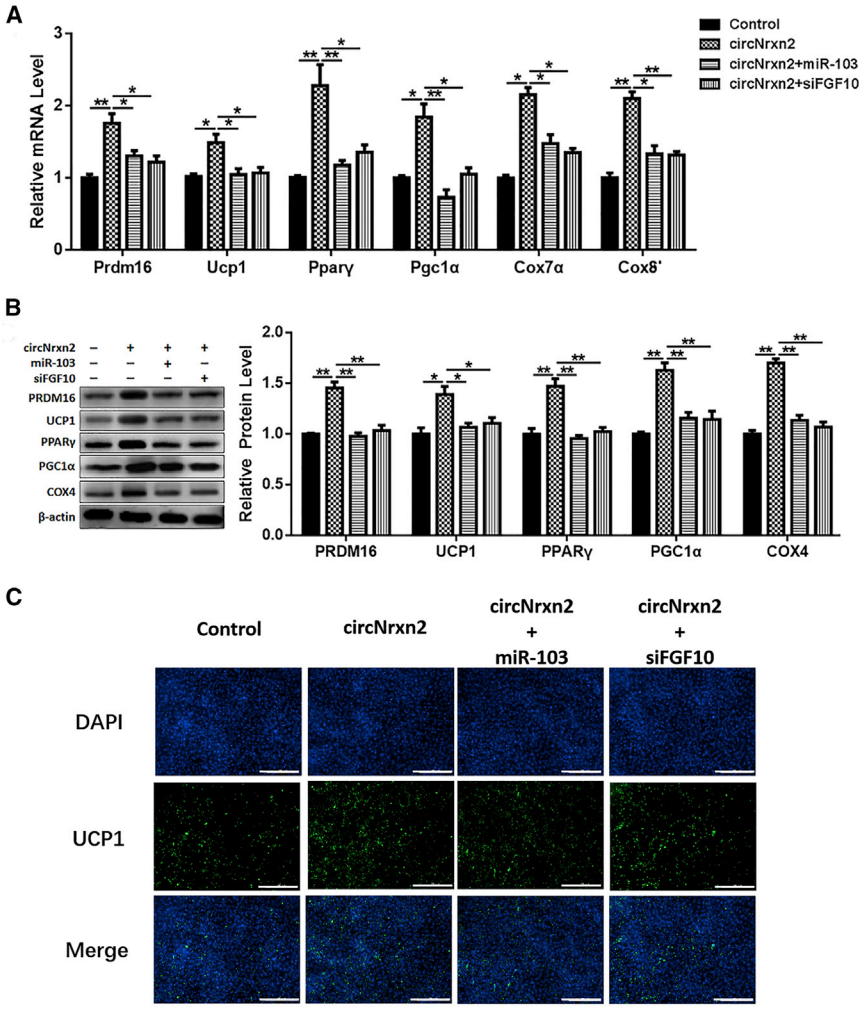

Figure 7. circNrxn2 Promoted White Adipocyte Browning by Increasing M2 Macrophage Polarization

RAW264.7 macrophages were treated with circNrxn2, circNrxn2 + mi-103, or circNrxn2 + siFGF10 and cultured for 24 h in 2% free fatty acid (FFA)-free BSA in 24-well plates, and the supernatant was collected as RAW-conditioned medium. 3T3-L1 adipocytes were incubated with RAW-conditioned medium for 24 h to detect mRNA expression levels and 48 h for protein levels. (A) The mRNA levels of PRDM16, UCP1, PPARγ, PGC1α, COX7α, and COX8b. (B) The protein levels of PRDM16, UCP1, PPARγ, PGC1α, and COX4. (C) Immunofluorescent staining of UCP1 in adipocytes. Data represent the mean ± SEM. Scale bars, 200 μm. *$p < 0.05$; **$p < 0.01$. $n \geq 3$.

tolerance to cold; therefore, it plays a role in cold-induced WAT browning in mice.[38] Moreover, miR-455 can also enhance the WAT browning response stimulated by cold and norepinephrine.[39] In contrast, several miRNA types were found to be negative regulators of WAT browning and BAT activity. miR-27 played a negative regulatory role in white fat browning.[40] miR-155 and C/EBPβ constituted a double closed-loop negative-feedback system that regulated the adipogenesis of brown or beige adipocytes.[41] miR-133 restricted the browning of adipocytes by inhibiting the transcription of the PRDM16.[42] Besides, researchers found that inhibition of the miR-327-FGF10-FGFR2 signaling axis can induce WAT browning and increase whole-body metabolic rate. They hypothesized that miRNAs targeting FGF10 would provide an effective new approach for the treatment of obesity and metabolic disorders.[43] What's more, it had been reported that fat-specific knockout of dicer, a target of miR-103, developed a loss of intra-abdominal and subcutaneous white fat and "whitening" of interscapular brown fat,[44] suggesting a potential role of miR-103 in the transformation of WAT and BAT. In this study, with bioinformatics predictive analysis, we found that circNrxn2 and FGF10 can specifically bind to miR-103, and we further explored their promotion of adipose tissue browning. Recent studies have also shown that adipocytes can interact with ATM by transporting miRNAs through vesicles,[45,46] so we wonder whether the browning of white adipocytes can also be activated by ATM.

Under normal circumstances, ATMs disperse in adipose tissue and participate in maintaining adipose tissue homeostasis. ATMs play a key role in the adipose tissue-liver crosstalk in nonalcoholic fatty liver diseases (NAFLDs). Our previous research also found that melatonin, a hormone, could divert adipose-derived exosomes to macrophages, which promoted M2 macrophage polarization to alleviate inflammation.[46] We also found that transcriptional factor Hoxa5 activated the PPARγ signaling pathway to increase M2 macrophage polarization, thereby ameliorating obesity-induced chronic fat inflammation. In obesity, the number of ATMs in WAT increased dramatically and mainly presented in M1 type, a coronal structure.[47] M1 macrophages were involved in the elimination of pathogens through the secretion of proinflammatory cytokines such as IL-6 and TNF-α. M2 macrophages inhibited inflammation and maintained physiological functions of adipose tissue. In addition to secreting the anti-inflammatory factor IL-10, adipose tissue M2 macrophages also played a key role in the browning of white fat. It was found that M2 macrophages secreted a large amount of norepinephrine (about 50% or more of the total) and induced WAT browning, promoted lipolysis, and increased thermogenesis after cold stimulation.[48] Studies have shown that specific knockout of RIP140 in monocytes and macrophages can promote the polarization of adipose tissue M2 macrophages, promote browning of WAT, and improve insulin sensitivity.[49] In addition, it was found that injection of M2 macrophages therapeutically induced WAT browning and improved HFD-induced insulin resistance.[50]

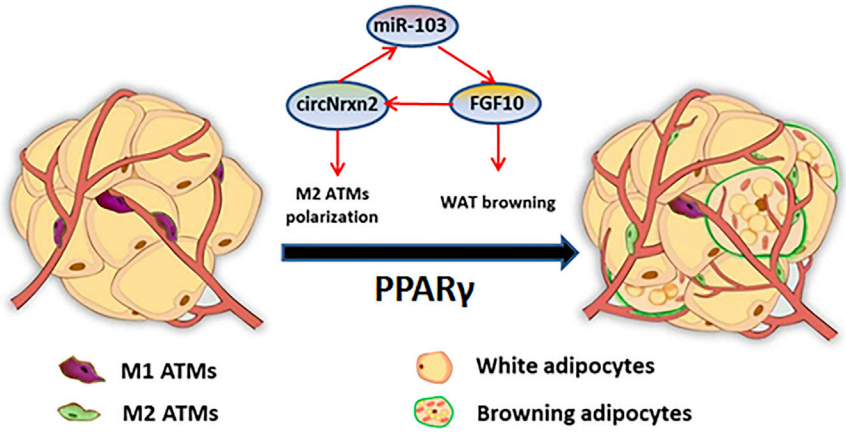

Figure 8. circNrxn2 Promoted WAT Browning by Facilitating M2 Macrophage Polarization
circNrxn2 acted as an endogenous miR-103 sponge and relieved the inhibitory effect of FGF10 to promote WAT browning via increasing M2 ATM polarization, which involved PPARγ activation.

The anti-hypertensive drug telmisartan could induce WAT browning by PPARγ-activation-mediated M2 polarization.[51] These studies showed that ATMs play a crucial role in body adipose metabolism. Besides, PPARγ had been reported as a master regulator of WAT browning and insulin sensitizer.[52,53] Here, we confirmed that circNrxn2 activated the PPARγ signaling pathway to promote WAT browning and increase M2 macrophage polarization.

However, there are still some limitations in our research. We find that a new ncRNA regulatory loop, circNrxn2-miR103-FGF10, could regulate WAT browning by affecting ATM polarization. However, it is unclear which specific regulatory factor in macrophages has an effect on WAT browning. Consistent with previous studies, we hypothesized that, due to our treatment, certain molecules in ATM are transported into adipocytes by exosomes and then cause browning. Based on this speculation, we next prepare to extract exosomes of ATM after treatment with circNrxn2, miR-103, and FGF10 and then search target molecules in ATMs that act on browning of adipocytes through proteomics sequencing. These experimental studies will be reflected in our future work.

Taken together, the data in our study revealed that circNrxn2 acted as an endogenous miR-103 sponge and relieved the inhibitory effect of FGF10 to promote WAT browning via increasing M2 macrophage polarization, which involved PPARγ activation (Figure 8). *In vivo*, we show that the delivery of circNrxn2 effectively promotes WAT browning and UCP1 expression in the HFD mice, demonstrating the functional impact of the circRNA on thermogenesis. Transfection of circNrxn2 alone can significantly increase FGF10 levels and promote browning of WAT. circNrxn2, miR-103, and FGF10 interacted with each other to form a regulatory loop in adipose tissue to regulate its browning. Nonetheless, this study provides a good therapeutic strategy for treating obesity and improving obesity-related metabolic disorders.

MATERIALS AND METHODS

Animal Experiments

Mice handling protocols were conducted following the guidelines and regulations approved by the Animal Ethics Committee of Northwest A&F University. C57BL/6J mice were purchased from the Laboratory Animal Center of the Fourth Military Medical University (Xi'an, China). Mice were housed at 25°C ± 1°C, 55% ± 5% humidity, in 12-h/12-h light/dark cycles and were provided with water and diet *ad libitum*. 8-week-old male mice were fed with a high fat diet (HFD; fat provides 60% of total energy) for 10 weeks to obtain obese mice.

HFD mice were housed at 4°C for 12 h to induce WAT browning. For *in vivo* studies, mice were treated with circNrxn2 lentiviruses, circNrxn2 lentiviruses + miR-103 adenoviruses, miR-103 adenoviruses, miR-103 adenoviruses + FGF10 adenoviruses, or control empty viruses at 1×10^9 plaque-forming units (PFUs) in 0.2 mL PBS through injection (i.p.) for 1 week, respectively. To remove macrophages, half of the mice received a daily injection i.p. of clodronate (Selleck, Shanghai, China), and the other half were injected with PBS.

Primary Cell Culture

The proposal of primary preadipocyte culture and differentiation was as described previously.[27,43] Primary peritoneal macrophages were obtained from 6-week-old C57BL/6J mice at 2–3 days after the injection of 2 mL 4% sterile thioglycolate solution by pelvic washing with PBS containing 3% fetal bovine serum (FBS). Primary cultures of macrophages were maintained in RPMI 1640 medium. All culture media were supplemented by the addition of 10% FBS and penicillin and streptomycin.

RNA Extraction and cDNA Synthesis

Total RNA, including miRNAs, was extracted using TRIzol Reagent (Invitrogen Life Technologies, Carlsbad, CA, USA). cDNA was synthesized using a PrimeScript II 1st Strand cDNA Synthesis Kit (Takara, Dalian, China).

qRT-PCR Analysis

qRT-PCR was used to detect the relative miRNA and mRNA levels with AceQ qRT-PCR SYBR Green Master Mix (Vazyme, Nanjing, China) as described by Cao et al.[44] U6 and GAPDH were used to normalize miRNA and mRNA levels, respectively. The relative gene expression was calculated using the $2^{-\Delta\Delta Ct}$ method.

Western Blot

Western blot analysis was performed by using standard methods as described by Liu et al.[45] Proteins were separated by

SDS-PAGE, transferred to polyvinylidene fluoride (PVDF) nitrocellulose membrane (Millipore, Boston, MA, USA), blocked with 5% fat-free milk for 2 h at room temperature, and then incubated with primary antibodies in 5% milk overnight at 4°C. Then, secondary antibody was added and incubated at room temperature for 2 h. Proteins were visualized using chemiluminescent peroxidase substrate (Millipore, Boston, MA, USA), and then the blots were quantified using the ChemiDoc XRS system (Bio-Rad, Hercules, CA, USA).

miRNA Target Genes and circRNA Prediction

To predict the miRNA target genes, we used three different bioinformatics software tools: TargetScan, miRBase, and PicTar. We chose their intersection to improve the accuracy of the forecast. circRNA prediction was performed in CircNet, circBase, starBase, and Circular RNA Interactome.

Biotin-Coupled miRNA Capture

Biotin-labeled wild-type (WT) or mutant (mut) miR-103 was transfected into adipocytes. 48 h after transfection, cells were collected and treated as described previously.[31]

Dual Luciferase Reporter Assay

Dual luciferase reporter assay proposal was performed as described by Liu et al.[45] For luciferase assay, renal luciferase expression plasmid (pRL-TK) vector and pGL3 vector containing a WT fragment of the 3′ UTRs of FGF10 or mutation fragment were transfected into 293T cells with miR-103 or circNrxn2. 48 h later, cells were harvested to analyze the luciferase activity using the Dual Luciferase Reporter Assay Kit (Promega, Madison, WI, USA).

Immunofluorescent Staining

Cells or tissue sections were fixed, permeabilized, and blocked. After incubating overnight with primary antibodies, secondary fluorescent antibodies were added, and DAPI was used for nuclear counterstaining.

Data Analysis

All experiments were repeated at least three times. Data were expressed as mean ± SEM. The statistical analysis of differences was performed in GraphPad Prism 5.0 using Student's t test. $^{*}p < 0.05$ was considered as statistical significance, and $^{**}p < 0.01$ means very significant.

SUPPLEMENTAL INFORMATION

Supplemental Information can be found online at https://doi.org/10.1016/j.omtn.2019.06.019.

AUTHOR CONTRIBUTIONS

Experimental design: T.Z. and C.S.; Performance of experiments: all authors; Data analysis: Z.Z. and T.X.; Writing the paper: T.Z. All authors are assured that we met the criteria for authorship, and all contributed to and reviewed the manuscript.

CONFLICTS OF INTERESTS

The authors declare no competing interests.

ACKNOWLEDGMENTS

This study was financially supported by Major National Scientific Research Projects (2015CB943102); the National Natural Science Foundation of China (31572365); the Joint Funds of the National Natural Science Foundation of China (U1804106); the Fundamental Research Funds for the Central Universities (245201971), the Key Sci-tech innovation team of Shaanxi province (2017KCT-24); and the Key Sci-tech innovation team of Northwest A&F University.

REFERENCES

1. Peirce, V., Carobbio, S., and Vidal-Puig, A. (2014). The different shades of fat. Nature *510*, 76–83.
2. Lee, Y.H., Jung, Y.S., and Choi, D. (2014). Recent advance in brown adipose physiology and its therapeutic potential. Exp. Mol. Med. *46*, e78.
3. Lackey, D.E., and Olefsky, J.M. (2016). Regulation of metabolism by the innate immune system. Nat. Rev. Endocrinol. *12*, 15–28.
4. Amit, I., Winter, D.R., and Jung, S. (2016). The role of the local environment and epigenetics in shaping macrophage identity and their effect on tissue homeostasis. Nat. Immunol. *17*, 18–25.
5. Zhou, Y., Yu, X., Chen, H., Sjöberg, S., Roux, J., Zhang, L., Ivoulsou, A.H., Bensaid, F., Liu, C.L., Liu, J., et al. (2015). Leptin deficiency shifts mast cells toward anti-inflammatory actions and protects mice from obesity and diabetes by polarizing M2 macrophages. Cell Metab. *22*, 1045–1058.
6. Dalmas, E., Toubal, A., Alzaid, F., Blazek, K., Eames, H.L., Lebozec, K., Pini, M., Hainault, I., Montastier, E., Denis, R.G., et al. (2015). Irf5 deficiency in macrophages promotes beneficial adipose tissue expansion and insulin sensitivity during obesity. Nat. Med. *21*, 610–618.
7. Wolf, Y., Boura-Halfon, S., Cortese, N., Haimon, Z., Sar Shalom, H., Kuperman, Y., Kalchenko, V., Brandis, A., David, E., Segal-Hayoun, Y., et al. (2017). Brown-adipose-tissue macrophages control tissue innervation and homeostatic energy expenditure. Nat. Immunol. *18*, 665–674.
8. Hui, X., Gu, P., Zhang, J., Nie, T., Pan, Y., Wu, D., Feng, T., Zhong, C., Wang, Y., Lam, K.S., and Xu, A. (2015). Adiponectin enhances cold-induced browning of subcutaneous adipose tissue via promoting M2 macrophage proliferation. Cell Metab. *22*, 279–290.
9. Barrett, S.P., Wang, P.L., and Salzman, J. (2015). Circular RNA biogenesis can proceed through an exon-containing lariat precursor. eLife *4*, e07540.
10. Starke, S., Jost, I., Rossbach, O., Schneider, T., Schreiner, S., Hung, L.H., and Bindereif, A. (2015). Exon circularization requires canonical splice signals. Cell Rep. *10*, 103–111.
11. Thomson, D.W., and Dinger, M.E. (2016). Endogenous microRNA sponges: evidence and controversy. Nat. Rev. Genet. *17*, 272–283.
12. Memczak, S., Jens, M., Elefsinioti, A., Torti, F., Krueger, J., Rybak, A., Maier, L., Mackowiak, S.D., Gregersen, L.H., Munschauer, M., et al. (2013). Circular RNAs are a large class of animal RNAs with regulatory potency. Nature *495*, 333–338.
13. Wang, K., Long, B., Liu, F., Wang, J.X., Liu, C.Y., Zhao, B., Zhou, L.Y., Sun, T., Wang, M., Yu, T., et al. (2016). A circular RNA protects the heart from pathological hypertrophy and heart failure by targeting miR-223. Eur. Heart J. *37*, 2602–2611.
14. Bartel, D.P. (2004). MicroRNAs: genomics, biogenesis, mechanism, and function. Cell *116*, 281–297.
15. Rupaimoole, R., and Slack, F.J. (2017). MicroRNA therapeutics: towards a new era for the management of cancer and other diseases. Nat. Rev. Drug Discov. *16*, 203–222.
16. Arner, P., and Kulyté, A. (2015). MicroRNA regulatory networks in human adipose tissue and obesity. Nat. Rev. Endocrinol. *11*, 276–288.

17. Deiuliis, J.A. (2016). MicroRNAs as regulators of metabolic disease: pathophysiologic significance and emerging role as biomarkers and therapeutics. Int. J. Obes. *40*, 88–101.

18. Kornfeld, J.W., Baitzel, C., Könner, A.C., Nicholls, H.T., Vogt, M.C., Herrmanns, K., Scheja, L., Haumaitre, C., Wolf, A.M., Knippschild, U., et al. (2013). Obesity-induced overexpression of miR-802 impairs glucose metabolism through silencing of Hnf1b. Nature *494*, 111–115.

19. Meerson, A., Traurig, M., Ossowski, V., Fleming, J.M., Mullins, M., and Baier, L.J. (2013). Human adipose microRNA-221 is upregulated in obesity and affects fat metabolism downstream of leptin and TNF-α. Diabetologia *56*, 1971–1979.

20. Rech, M., Kuhn, A.R., Lumens, J., Carai, P., van Leeuwen, R., Verhesen, W., Verjans, R., Lecomte, J., Liu, Y., Luiken, J.J.F.P., et al. (2019). AntagomiR-103 and -107 treatment affects cardiac function and metabolism. Mol. Ther. Nucleic Acids *14*, 424–437.

21. Trajkovski, M., Hausser, J., Soutschek, J., Bhat, B., Akin, A., Zavolan, M., Heim, M.H., and Stoffel, M. (2011). MicroRNAs 103 and 107 regulate insulin sensitivity. Nature *474*, 649–653.

22. Martello, G., Rosato, A., Ferrari, F., Manfrin, A., Cordenonsi, M., Dupont, S., Enzo, E., Guzzardo, V., Rondina, M., Spruce, T., et al. (2010). A microRNA targeting dicer for metastasis control. Cell *141*, 1195–1207.

23. Chen, H.Y., Lin, Y.M., Chung, H.C., Lang, Y.D., Lin, C.J., Huang, J., Wang, W.C., Lin, F.M., Chen, Z., Huang, H.D., et al. (2012). miR-103/107 promote metastasis of colorectal cancer by targeting the metastasis suppressors DAPK and KLF4. Cancer Res. *72*, 3631–3641.

24. Wang, J.X., Zhang, X.J., Li, Q., Wang, K., Wang, Y., Jiao, J.Q., Feng, C., Teng, S., Zhou, L.Y., Gong, Y., et al. (2015). MicroRNA-103/107 regulate programmed necrosis and myocardial ischemia/reperfusion injury through targeting FADD. Circ. Res. *117*, 352–363.

25. Li, M., Liu, Z., Zhang, Z., Liu, G., Sun, S., and Sun, C. (2015). miR-103 promotes 3T3-L1 cell adipogenesis through AKT/mTOR signal pathway with its target being MEF2D. Biol. Chem. *396*, 235–244.

26. Zhang, Z., Wu, S., Muhammad, S., Ren, Q., and Sun, C. (2018). miR-103/107 promote ER stress-mediated apoptosis via targeting the Wnt3a/β-catenin/ATF6 pathway in preadipocytes. J. Lipid Res. *59*, 843–853.

27. Zhang, Z., Zhang, T., Feng, R., Huang, H., Xia, T., and Sun, C. (2019). circARF3 alleviates mitophagy-mediated inflammation by targeting miR-103/TRAF3 in mouse adipose tissue. Mol. Ther. Nucleic Acids *14*, 192–203.

28. Dempersmier, J., Sambeat, A., Gulyaeva, O., Paul, S.M., Hudak, C.S., Raposo, H.F., Kwan, H.Y., Kang, C., Wong, R.H., and Sul, H.S. (2015). Cold-inducible Zfp516 activates UCP1 transcription to promote browning of white fat and development of brown fat. Mol. Cell *57*, 235–246.

29. Ohno, H., Shinoda, K., Spiegelman, B.M., and Kajimura, S. (2012). PPARγ agonists induce a white-to-brown fat conversion through stabilization of PRDM16 protein. Cell Metab. *15*, 395–404.

30. Odegaard, J.I., Ricardo-Gonzalez, R.R., Goforth, M.H., Morel, C.R., Subramanian, V., Mukundan, L., Red Eagle, A., Vats, D., Brombacher, F., Ferrante, A.W., and Chawla, A. (2007). Macrophage-specific PPARgamma controls alternative activation and improves insulin resistance. Nature *447*, 1116–1120.

31. Sanchez-Gurmaches, J., and Guertin, D.A. (2014). Adipocytes arise from multiple lineages that are heterogeneously and dynamically distributed. Nat. Commun *19*, 4099.

32. Wu, J., Boström, P., Sparks, L.M., Ye, L., Choi, J.H., Giang, A.H., Khandekar, M., Virtanen, K.A., Nuutila, P., Schaart, G., et al. (2012). Beige adipocytes are a distinct type of thermogenic fat cell in mouse and human. Cell *150*, 366–376.

33. Milet, C., Bléher, M., Allbright, K., Orgeur, M., Coulpier, F., Duprez, D., and Havis, E. (2017). Egr1 deficiency induces browning of inguinal subcutaneous white adipose tissue in mice. Sci. Rep. *7*, 16153.

34. Stefanidis, A., Wiedmann, N.M., Tyagi, S., Allen, A.M., Watt, M.J., and Oldfield, B.J. (2018). Insights into the neurochemical signature of the innervation of beige fat. Mol. Metab. *11*, 47–58.

35. Paschos, G.K., Tang, S.Y., Theken, K.N., Li, X., Verginadis, I., Lekkas, D., Herman, L., Yan, W., Lawson, J., and FitzGerald, G.A. (2018). Cold-induced browning of inguinal white adipose tissue is independent of adipose tissue cyclooxygenase-2. Cell Rep. *24*, 809–814.

36. Hansen, T.B., Jensen, T.I., Clausen, B.H., Bramsen, J.B., Finsen, B., Damgaard, C.K., and Kjems, J. (2013). Natural RNA circles function as efficient microRNA sponges. Nature *495*, 384–388.

37. John, E., Wienecke-Baldacchino, A., Liivrand, M., Heinäniemi, M., Carlberg, C., and Sinkkonen, L. (2012). Dataset integration identifies transcriptional regulation of microRNA genes by PPARγ in differentiating mouse 3T3-L1 adipocytes. Nucleic Acids Res. *40*, 4446–4460.

38. Ng, R., Hussain, N.A., Zhang, Q., Chang, C., Li, H., Fu, Y., Cao, L., Han, W., Stunkel, W., and Xu, F. (2017). miRNA-32 drives brown fat thermogenesis and trans-activates subcutaneous white fat browning in mice. Cell Rep. *19*, 1229–1246.

39. Zhang, H., Guan, M., Townsend, K.L., Huang, T.L., An, D., Yan, X., Xue, R., Schulz, T.J., Winnay, J., Mori, M., et al. (2015). MicroRNA-455 regulates brown adipogenesis via a novel HIF1an-AMPK-PGC1α signaling network. EMBO Rep. *16*, 1378–1393.

40. Lee, J.Y., Takahashi, N., Yasubuchi, M., Kim, Y.I., Hashizaki, H., Kim, M.J., Sakamoto, T., Goto, T., and Kawada, T. (2012). Triiodothyronine induces UCP-1 expression and mitochondrial biogenesis in human adipocytes. Am. J. Physiol. Cell Physiol. *302*, C463–C472.

41. López, M., Diéguez, C., and Nogueiras, R. (2015). Hypothalamic GLP-1: the control of BAT thermogenesis and browning of white fat. Adipocyte *4*, 141–145.

42. Lone, J., Choi, J.H., Kim, S.W., and Yun, J.W. (2016). Curcumin induces brown fat-like phenotype in 3T3-L1 and primary white adipocytes. J. Nutr. Biochem. *27*, 193–202.

43. Fischer, C., Seki, T., Lim, S., Nakamura, M., Andersson, P., Yang, Y., Honek, J., Wang, Y., Gao, Y., Chen, F., et al. (2017). A miR-327-FGF10-FGFR2-mediated autocrine signaling mechanism controls white fat browning. Nat. Commun. *8*, 2079.

44. Mori, M.A., Thomou, T., Boucher, J., Lee, K.Y., Lallukka, S., Kim, J.K., Torriani, M., Yki-Järvinen, H., Grinspoon, S.K., Cypess, A.M., and Kahn, C.R. (2014). Altered miRNA processing disrupts brown/white adipocyte determination and associates with lipodystrophy. J. Clin. Invest. *124*, 3339–3351.

45. Ying, W., Riopel, M., Bandyopadhyay, G., Dong, Y., Birmingham, A., Seo, J.B., Ofrecio, J.M., Wollam, J., Hernandez-Carretero, A., Fu, W., et al. (2017). Adipose tissue macrophage-derived exosomal miRNAs can modulate in vivo and in vitro insulin sensitivity. Cell *171*, 372–384.e12.

46. Liu, Z., Gan, L., Zhang, T., Ren, Q., and Sun, C. (2018). Melatonin alleviates adipose inflammation through elevating α-ketoglutarate and diverting adipose-derived exosomes to macrophages in mice. J. Pineal Res. *64*, e12455.

47. Gandotra, S., Le Dour, C., Bottomley, W., Cervera, P., Giral, P., Reznik, Y., Charpentier, G., Auclair, M., Delépine, M., Barroso, I., et al. (2011). Perilipin deficiency and autosomal dominant partial lipodystrophy. N. Engl. J. Med. *364*, 740–748.

48. Nguyen, K.D., Qiu, Y., Cui, X., Goh, Y.P., Mwangi, J., David, T., Mukundan, L., Brombacher, F., Locksley, R.M., and Chawla, A. (2011). Alternatively activated macrophages produce catecholamines to sustain adaptive thermogenesis. Nature *480*, 104–108.

49. Liu, P.S., Lin, Y.W., Lee, B., McCrady-Spitzer, S.K., Levine, J.A., and Wei, L.N. (2014). Reducing RIP140 expression in macrophage alters ATM infiltration, facilitates white adipose tissue browning, and prevents high-fat diet-induced insulin resistance. Diabetes *63*, 4021–4031.

50. Liu, P.S., Lin, Y.W., Burton, F.H., and Wei, L.N. (2015). Injecting engineered anti-inflammatory macrophages therapeutically induces white adipose tissue browning and improves diet-induced insulin resistance. Adipocyte *4*, 123–128.

51. Jeon, E.J., Kim, D.Y., Lee, N.H., Choi, H.E., and Cheon, H.G. (2019). Telmisartan induces browning of fully differentiated white adipocytes via M2 macrophage polarization. Sci. Rep. *9*, 1236.

52. Ahmadian, M., Suh, J.M., Hah, N., Liddle, C., Atkins, A.R., Downes, M., and Evans, R.M. (2013). PPARγ signaling and metabolism: the good, the bad and the future. Nat. Med. *19*, 557–566.

53. García-Alonso, V., López-Vicario, C., Titos, E., Morán-Salvador, E., González-Périz, A., Rius, B., Párrizas, M., Werz, O., Arroyo, V., and Clària, J. (2013). Coordinate functional regulation between microsomal prostaglandin E synthase-1 (mPGES-1) and peroxisome proliferator-activated receptor γ (PPARγ) in the conversion of white-to-brown adipocytes. J. Biol. Chem. *288*, 28230–28242.